Earthquake Geotechnical Engineering for Protection and Development of Environment and Constructions – Silvestri & Moraci (Eds)
© 2019 Associazione Geotecnica Italiana, Rome, Italy, ISBN 978-0-367-14328-2

Extension of the procedure for evaluating parameters of strike–slip fault with surface breakings for strong motion prediction

K. Dan & A. Oana
Ohsaki Research Institute, Inc., Japan

H. Fujiwara & N. Morikawa
National Research Institute for Earth Science and Disaster Resilience, Japan

ABSTRACT: Dan et al. (2011) proposed a procedure for evaluating parameters of long strikeslip faults for strong motion prediction. Recently, Dan et al. (2019) validated this procedure by reproducing the strong ground motions observed during the 1999 Kocaeli, Turkey, earthquake. However, the procedure does not take the shallow part of the fault above the seismogenic layer into account, and therefore it can not reproduce permanent displacements along the fault traces. On the other hand, Ikutama et al. (2018) proposed a procedure for modeling the shallow part of the fault, and reproduced the strong ground motions, including the permanent displacements, observed during the 2016 Kumamoto, Japan, earthquake. In this paper, we extended the procedure of Dan et al. (2011) to the shallow part of the fault by adding the procedure of Ikutama et al. (2018), and reproduced the strong ground motions and the permanent displacements of the Kumamoto earthquake.

1 INTRODUCTION

The Headquarters for Earthquake Research Promotion (2005) compiled a procedure, called Recipe, for evaluating fault parameters for strong motion prediction, and it has been adopted as a guideline in Japan. This Recipe works well for moderate-sized earthquakes. However, it estimates unrealistic fault parameters for long faults, and suggests a tentative procedure for these cases. Hence, Dan *et al*. (2011) proposed a procedure, as an alternative guideline, for evaluating fault parameters of asperity models for predicting strong ground motions from crustal earthquakes caused by long strike-slip faults.

In order to validate this procedure, Dan *et al*. (2019) made an asperity model for a strike-slip fault 141 km long in accordance with this procedure, predicted ground motions by the stochastic Green's function method, and showed that the PGA's, PGV's, predicted velocity motions, and pseudo velocity response spectra, agreed well with the observed ones in the 1999 Kocaeli, Turkey, earthquake (M_W 7.6). In their calculation, the shallow part of the fault in the surface layers was not modeled, although clear fault traces were observed in the Kocaeli earthquake. This is because the Headquarters for Earthquake Research Promotion (2005) assumes that the shallow part of the fault in the surface layers is broken by the movement of the deep part of the fault in the seismogenic layer and that modeling of the deep part is sufficient for predicting strong ground motions. Recently, Ikutama *et al*. (2018) modeled both the deep part and the shallow part of the fault to reproduce permanent displacements at the sites very close to the fault trace of the 2016 Kumamoto, Japan, earthquake.

Accordingly, we extended the procedure of Dan *et al*. (2011) to include the shallow part of the fault to predict permanent displacements near the fault traces.

2 MODELING OF FAULTS OF CRUSTAL EARTHQUAKES WITH SURFACE BREAKINGS

We modeled the entire ruptured fault from the ground surface to the bottom of the seismogenic layer. Hereafter, the fault area between the top and the bottom of the seismogenic layer designates the deep part of the fault (seismic fault), and the fault area from the ground surface to the top of the seismogenic layer designates the shallow part of the fault.

2.1 *Modeling of the deep part of the fault in the seismogenic layer*

Dan *et al.* (2011) proposed a procedure for evaluating the fault parameters of deep parts (seismic faults) of long vertical strike-slip faults.

In their procedure, the length of the active fault L_{act}, the dip δ, and the upper depth dep_1 and lower depth dep_2 of the seismogenic layer are assumed a priori based on the information obtained by geological survey and seismological investigation. Then, the length of the surface fault L_{sur} is set to be L_{sur}=L_{act}, and the length of the seismic fault L_{seis} is also set to be L_{seis}=L_{act}. The entire fault width W is W=dep_2/sinδ, and the seismic fault width W_{seis} is W_{seis}=(dep_2-dep_1)/sinδ.

The reasonings and more detailed explanation is given in Dan *et al.* (2019).

2.1.1 *Slip velocity time function on the deep part of the fault*

We adopted the approximate function by Nakamura & Miyatake (2000) as the slip velocity time function on the deep part of the fault according to the Headquarters for Earthquake Research Promotion (2005). This function is expressed by equation (23) in IAEA (2015).

2.1.2 *Slip on the deep part of the fault*

There are three kinds of slips on the deep part of the fault: the averaged slip all over the deep part of the fault D_{seis}, the averaged slip on the asperities D_{asp}, and the slip on the background D_{back}. We explain below how the procedure evaluates these three kinds of slips.

a) averaged slip all over the deep part of the fault

The averaged slip all over the deep part of the fault D_{seis} can be calculated by

$$D_{seis} = M_0/\mu S_{seis}. \tag{1}$$

Here, M_0 is the seismic moment, evaluated by

$$M_0 = (\Delta\sigma^{\#} S_{seis} W_{seis})/(0.5 + 2\exp[-L_{seis}/W_{seis}]), \tag{2}$$

Where μ is the rigidity at the source, and S_{seis} is the seismic fault area, given by

$$S_{seis} = L_{seis} W_{seis}. \tag{3}$$

b) averaged slip on the asperities

From Somerville *et al.* (1999), the averaged slip on the asperities D_{asp} is calculated by

$$D_{asp} = 2D_{seis}. \tag{4}$$

c) slip on the background

The slip on the background D_{back} is calculated by

$$D_{back} = (S_{seis} D_{seis} - S_{asp} D_{asp})/S_{back}. \tag{5}$$

Here, S_{asp} is the asperity area, given by

$$S_{asp} = (\Delta\sigma^{\#}/\Delta\sigma^{\#}_{asp}) S_{seis}, \tag{6}$$

and S_{back} is the background area, given by

$$S_{back} = S_{seis} - S_{asp}. \tag{7}$$

2.1.3 *Maximum slip velocity on the deep part of the fault*

The maximum slip velocity V_{max} of the approximate function by Nakamura & Miyatake (2000) is given by

$$V_{max} = \Delta\sigma(2f_c W V_r)^{1/2}/\mu. \tag{8}$$

Here, $\Delta\sigma$ is the stress drop, f_c is the cut-off frequency, W is the width of the asperity or background, and V_r is the rupture propagation velocity.

2.2 *Model of the deep part of the fault of the 2016 Kumamoto earthquake*

The Headquarters for Earthquake Research Promotion (2013) proposed the bottom of the seismogenic layer is 17 km deep in the area of the Kumamoto earthquake, and National Institute of Advanced Industrial Science and Technology (2016) observed the surface fault of 34 km in the 2016 Kumamoto earthquake, consisting of 28-km long Futagawa segment and 6-km long Hinagu segment. Accordingly, we assumed both the surface fault length L_{sur} and the seismic fault length L_{seis} to be 34 km, and the fault width W to be 18.8 km for Futagawa segment dipping 65 degrees and to be 17.9 km for Hinagu segment dipping 72 degrees. We assumed the upper depth of the seismogenic layer to be 3 km (Headquarters for Earthquake Research Promotion, 2014).

All the parameters of the deep part of the fault were evaluated by the existing procedure of Dan *et al.* (2011). We adopted the strikes, the dips, and the rakes of the segments in Oana *et al.* (2017), and we also decided the locations of the asperities based on Oana *et al.* (2017).

Table 1 lists the model parameters of the deep part of the fault of the 2016 Kumamoto earthquake. Figure 1 compares the existing SMGA (strong motion generation area) model for the 2016 Kumamoto earthquake by Oana *et al.* (2017) shown by the black line with the deep part of the fault model proposed in this study shown by the blue line.

Figure 2 shows the model of the deep part of the fault (seismic fault in the seismogenic layer) for the 2016 Kumamoto earthquake by the existing procedure of Dan *et al.* (2011), and Figure 3 shows the slip velocity time functions on the deep part of the fault.

2.3 *Modeling of the shallow part of the fault in the surface layers*

Similarly to Ikutama *et al.* (2018), we set two kinds of areas in the shallow part of the fault: a large-slip area and a small-slip area. A large-slip area is located just above the asperity in the deep part of the fault, and a small-slip area is located above the background in the deep part.

Table 1. Model parameters of the deep part of the fault of the 2016 Kumamoto earthquake evaluated by the existing procedure of Dan *et al.* (2011).

		this study	2016 Kumamoto earthquake
surface fault length L	km	34	34
fault width W	km	18.8, 17.9	18
seismic moment M_0	Nm	3.78E+19	4.42E+19*1
averaged dynamic stress drop $\Delta\sigma$	MPa	3.4	-
short-period level A	Nm/s^2	1.20E+19	1.21E+19*2
asperity area ratio γ_s		0.28	-
asperity area S_{asp}	km^2	145	-
averaged slip on the asperities D_{asp}	m	4.7	3～5*3
asperity stress drop $\Delta\sigma_{asp}$	MPa	12.2	11.5*4

*1) F-net. *2) Average of the short-period levels by Satoh (2017), Irikura *et al.*(2017), Nakano and Kawase (2016), and Oana *et al.* (2017). *3) Oana *et al.* (2017). *4) Average of the stress drops on SMGA's in the Futagawa segment by Satoh (2017), Irikura *et al.* (2017), and Oana *et al.* (2017).

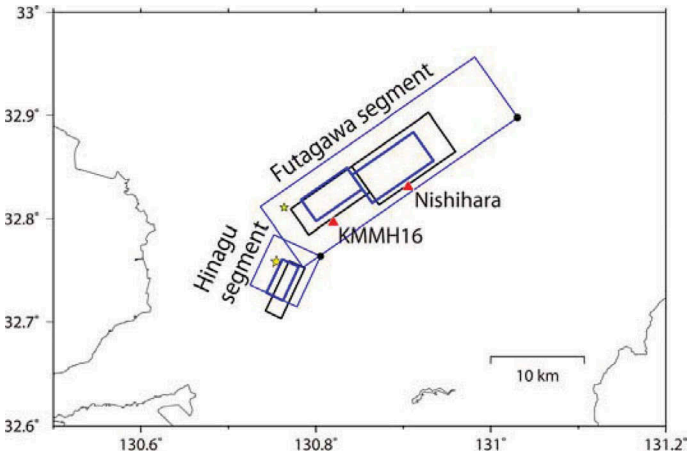

Figure 1. Comparison of the existing SMGA model for the 2016 Kumamoto earthquake of Oana *et al.* (2017) shown by the black line with the deep part of the fault model proposed in this study shown by the blue line.

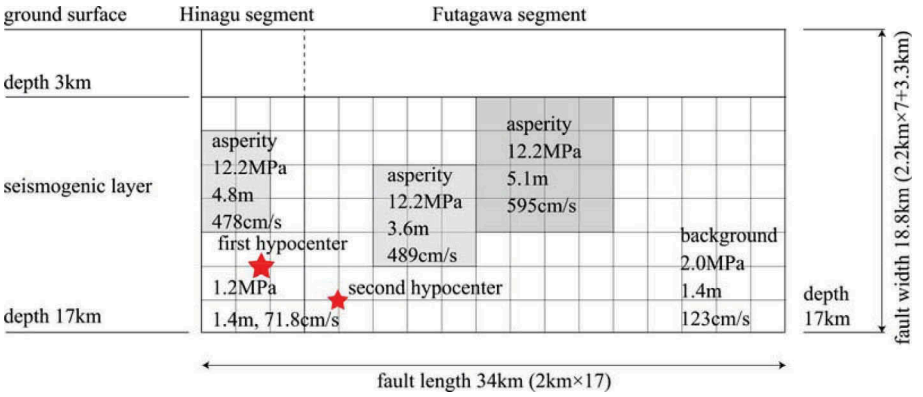

Figure 2. Model of the deep part of the fault (seismic fault in the seismogenic layer) for the 2016 Kumamoto earthquake by the existing procedure of Dan et al. (2011).

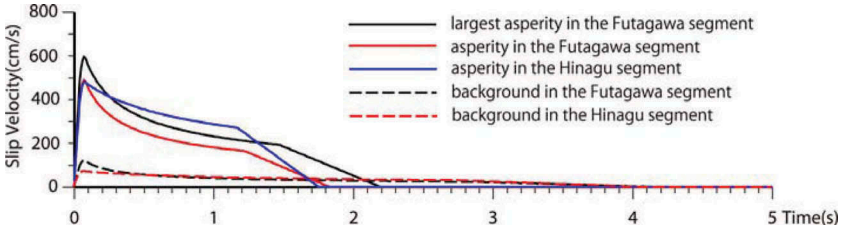

Figure 3. Slip velocity time functions on the deep part of the fault.

2.3.1 *Slip velocity time function on the shallow part of the fault*

We used a triangular shape as the slip velocity time function on the shallow part of the fault, instead of the approximate function by Nakamura & Miyatake (2000), similarly to Ikutama *et al.* (2018).

2.3.2 *Slip on the shallow part of the fault*

a) Slip on the large-slip area

There are three alternatives to evaluate the slip on the large-slip area.

The first option is to use displacement obtained from geological surveys, which is unique for each individual earthquake.

The second option is to adopt empirical relationships between the maximum slip on the fault trace and the fault length (*e.g.* Matsuda, 1975; Wells & Coppersmith, 1994). In this paper, we adopted the empirical relationship given by Matsuda (1975). Here, the magnitude M is set by equation (9) from the length L_{sur} of the fault, and then the slip D_{large} is obtained by equation (10) from the magnitude M.

$$\log L_{sur} = 0.6M - 2.9 \tag{9}$$

$$\log D_{large} = 0.6M - 4.0 \tag{10}$$

The third option is to use the empirical relationship based on the findings of Matsushima *et al.* (2010), which describes a relationship of the maximum slip on the fault trace and the averaged slip on the seismic fault. Matsushima *et al.* (2010) indicated that the empirical relationship between the maximum displacement observed on the fault trace and the average slip over the fault plane is a factor of 2-3 for a long fault. We can use this empirical relationship to determine the slip for the large-slip area as 1-1.5 times the slip on the asperity, because the slip on the asperity is twice the averaged slip on the fault according to Somerville *et al.* (1999).

b) Slip on the small-slip area

We assumed the slip on the small-slip area D_{small} to be evaluated by the proportional relation among D_{large}, D_{small}, D_{asp}, and D_{back} as follows:

$$D_{small} = D_{large}\,(D_{back}/D_{asp}). \tag{11}$$

2.3.3 *Maximum slip velocity on the shallow part of the fault*

As Kagawa *et al.* (2004) showed that the averaged slip velocity on shallow asperities was about half the averaged slip velocity on deep asperities, we set the maximum slip velocity on the large-slip area in the shallow part of the fault to half the maximum slip velocity on the asperity in the deep part of the fault. Also, the maximum slip velocity on the small-slip area can be set to half the maximum slip velocity on the background.

2.4 *Model of the shallow part of the fault of the 2016 Kumamoto earthquake*

We assigned a large-slip area just above the largest asperity and a small-slip area above the background in the Futagawa segment, and another small-slip area above the background in the Hinagu segment, as shown in Figure 4.

As for the slip on the large-slip area D_{large}, we chose the third option of using the results by Matsushima *et al.* (2010), and set it to be the same value of the slip of 5.1 m on the largest asperity D_{asp}. Then, the slip on the small-slip area D_{small} was calculated to be 1.4 m by equation (11).

Figure 4 shows the model of the entire ruptured fault for the 2016 Kumamoto earthquake by the extended procedure of this study, and Figure 5 shows the slip velocity time functions for the shallow part of the fault.

Note here that the seismic moment calculated by equation (2) does not include the seismic moment of the shallow part of the fault, which would be 10 to 15% of it when the rigidity of the surface layer is half the rigidity of the seismogenic layer.

2.5 *Other fault parameters*

We adopted a multi-hypocenter model *i.e.* one hypocenter in each segment, and assumed a radial rupture propagation in each segment, as Oana *et al.* (2017) did. The rupture

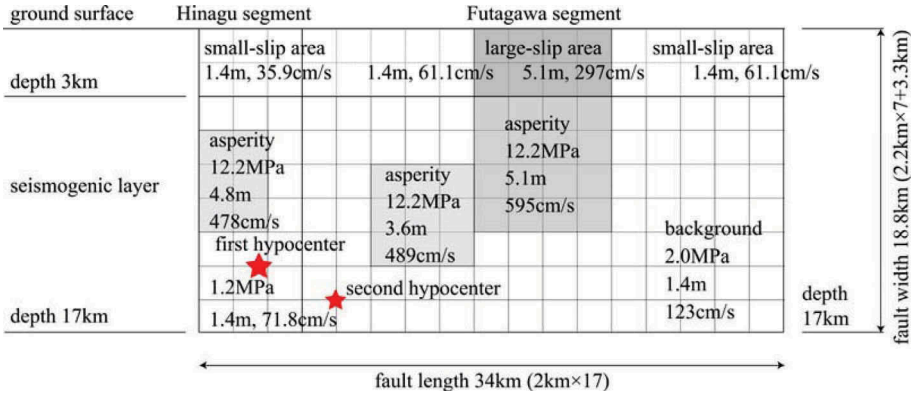

Figure 4. Model of the entire ruptured fault for the 2016 Kumamoto earthquake by the extended procedure of this study.

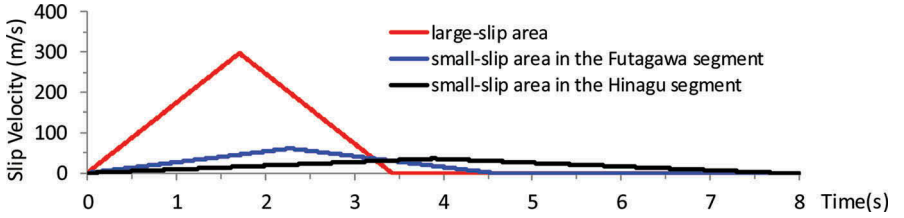

Figure 5. Slip velocity time functions for the shallow part of the fault.

propagation velocity was set to 3.0 km/s on the larger asperity in the Futagawa segment and the asperity in the Hinagu segment and 2.7 km/s on the rest of the fault.

3 METHOD OF CALCULATING GROUND MOTIONS

3.1 *Ground motions from the deep part of the fault*

We calculated the strong ground motions from the deep part of the fault by the hybrid method (Kamae *et al.*, 1998), combining the results in the shorter period range by the stochastic Green's function method (Boore, 1983) and those in the longer period range by the wavenumber integration method (Hisada & Bielak, 2003).

3.2 *Ground motions from the shallow part of the fault*

The shallow fault is an area that is not modeled by the Recipe for strong ground motion prediction because the rupture in this area occurs passively in association with the deep fault slip, and that there is no autonomous rupture. Consequently, we assumed the stress drop to be zero on the shallow part and calculated the ground motions by the wavenumber integration method because the effects of the shallow part appear in the long period range.

We set the calculated minimum period to be 0.32 s (3.125 Hz), and the number of Gauss points per fault element for fault surface integration was 6 (6×6=36 points).

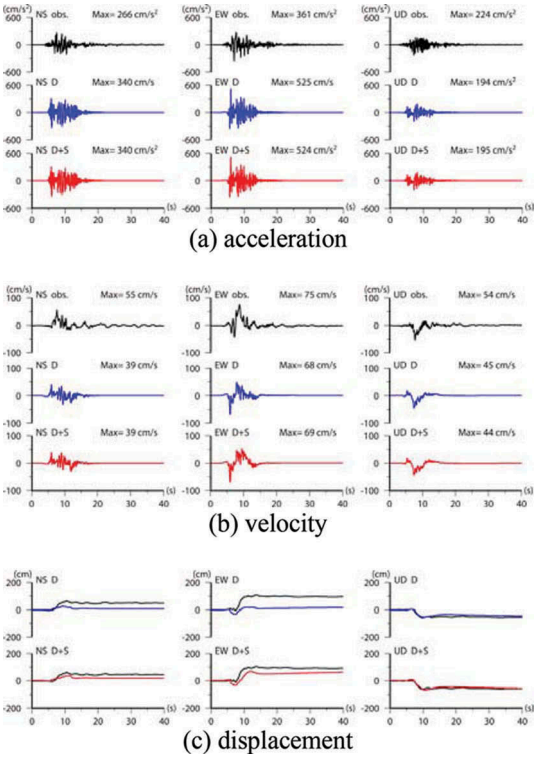

Figure 6. Comparison of the calculated motions with the observed motions at Mashiki station (KMMH16) 2km away from the fault trace (obs: observed, D: deep part only, D+S: deep and shallow parts)

3.3 *Ground motions from the entire fault*

We superimposed the motions from the deep part of the fault and those from the shallow part of the fault in the time domain.

4 CALCULATED GROUND MOTIONS

We calculated ground motions at two stations: Mashiki station, 2 km away from the fault trace, and Nishihara station, 700 m away from the fault trace.

4.1 *Results at Mashiki station 2 km away from the fault trace*

It is found out that the observed accelerations, velocities, and displacements are reproduced very well with and without the shallow part of the fault.

4.2 *Results at Nishihara station 700 m away from the fault trace*

We find that the observed accelerations are reproduced very well with and without the shallow part of the fault. However, the observed velocities and displacements are not reproduced well without the shallow part of the fault, while they are reproduced well when the shallow part is included.

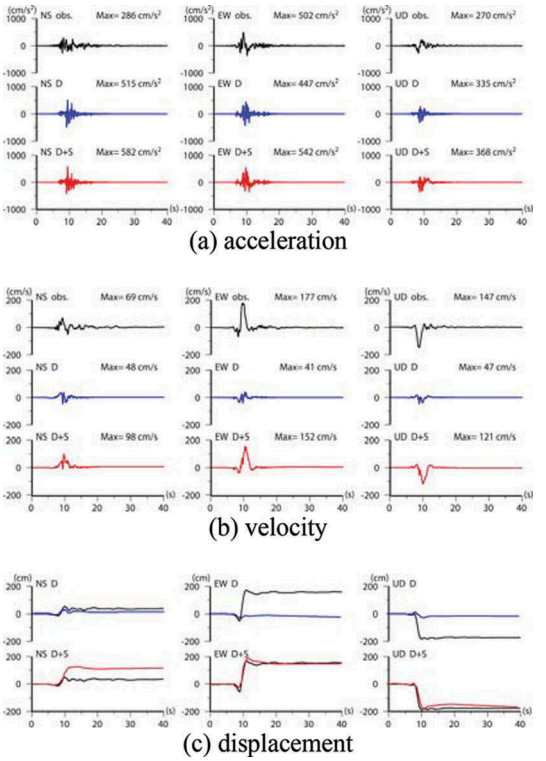

Figure 7. Comparison of the calculated motions with the observed motions at Nishihara station 700 m away from the fault trace (obs: observed, D: deep part only, D+S: deep and shallow parts)

5 CONCLUSIONS

We extended the procedure for evaluating parameters of long strike-slip faults by Dan *et al.* (2011) to include the shallow part of the fault. The original existing procedure could reproduce the observed accelerations, velocities, and displacements at Mashiki station, 2 km from the fault trace and the observed accelerations at Nishihara station, 700 m from the fault. But it underestimated the observed velocities and displacements at Nishihara stations. Meanwhile, the extended procedure could reproduce the observed velocities and displacements, including the permanent displacements, as well as the observed accelerations, both at Mashiki station and Nishihara station.

ACKNOWLEDGMENTS

The authors appreciate Japan Meteorological Agency, Kumamoto Prefecture, and National Research Institute for Earth Science and Disaster Resilience for providing the ground motion records.

REFERENCES

Boore, D. M. 1983. Stochastic simulation of high-frequency ground motions based on seismological models of the radiated spectra, *Bulletin of the Seismological Society of America* 73: 1865-1894.

Dan, K., Ju, D., Irie, K., Arzpeima, S. & Ishii, Y. 2011. Estimation of averaged dynamic stress drops of inland earthquakes caused by long strike-slip faults and its application to asperity models for

predicting strong ground motions, *Journal of Structural and Construction Engineering (Transactions of the Architectural Institute of Japan) AIJ* 670: 2041-2050 (in Japanese with English abstract).
Dan, K., Ju, D., Fujiwara, H. & Morikawa, N. 2019. Validation of the new procedures for evaluating parameters of crustal earthquakes caused by long faults for ground motion prediction, *Bulletin of the Seismological Society of America* 109(1),152-163.
Headquarters for Earthquake Research Promotion. 2005. *Map of Predicted Earthquake Ground Motions in Japan* (in Japanese).
Headquarters for Earthquake Research Promotion. 2013. https://www.jishin.go.jp/main/chousa/katsudan sou_pdf/93_futagawa_hinagu_2.pdf, 2013 (referred on July 12, 2017)
Headquarters for Earthquake Research Promotion: Notional Seismic Hazard Maps for Japan, 2014.
Hisada, Y. & Bielak, J. 2003. A theoretical method for computing near-fault ground motions in layered half-spaces considering static offset due to surface faulting, with a physical interpretation of fling step and rupture directivity, *Bulletin of the Seismological Society of America* 93(3): 1154–1168.
IAEA. 2015. Ground Motion Simulation Based on Fault Rupture Modelling for Seismic Hazard Assessment in Site Evaluation for Nuclear Installations, *Safety Report Series* 85.
Ikutama, S., Kawasato, T., Kawakami, Y., Nohsho, M., Oana, A., Dan, K., Torita, H. & Okada, Y. 2018. Source modeling for predicting ground motions and permanent displacements very close to the fault trace, *Journal of Earthquake and Tsunami* 12, Vol.12,No.4, DOI:10.1142/S1793431118410051.
Kagawa, T., Irikura, K. & Somerville, P. G. 2004. Differences in ground motion and fault rupture process between the surface and buried rupture earthquakes, *Earth, Planets and Space* 56: 3-14.
Kamae, K., Irikura, K. & Pitarka, A. 1998. A technique for simulating strong ground motion using hybrid Green's function, *Bulletin of the Seismological Society of America* 88(2): 357-367.
Matsuda, T. 1975. Magnitude and recurrence interval of earthquakes from a fault, *Journal of the Seismological Society of Japan, Second Series* 28 (3):269-283 (in Japanese with English abstract).
Matsushima, S., Murotani, S., Azuma, T., Irikura, K. & Kitagawa, S. 2010. Scaling relations of earthquakes on active mega-fault systems, *Geophysical Bulletin of Hokkaido University* 73: 117-127 (in Japanese with English abstract).
Nakamura, H. & Miyatake, T. 2000. An approximate expression of slip velocity time function for simulation of near-field strong ground motion, *Journal of the Seismological Society of Japan, Second Series* 53: 1-9 (in Japanese).
National Institute of Advanced Industrial Science and Technology Geological Survey of Japan). https:// www.gsj.jp/hazards/earthquake/kumamoto2016/kumamoto20160513-1.html, 2016 (referred on July 12, 2017)
Oana, A., Dan, K., Miyakoshi, J., Fujiwara, H., Morikawa, N. & Maeda, T. 2017. Estimation of characterized source model of the mainshock in the 2016 Kumamoto earthquakes using the stochastic Green's function method, *Japan Geoscience Union Meeting 2017* SCG70-P04.
Somerville, P. G., Irikura, K., Graves, R., Sawada, S., Wald, D., Abrahamson, N., Iwasaki, Y., Kagawa, T., Smith, N. & Kowada, A. 1999. Characterizing crustal earthquake slip models for the prediction of strong ground motion, *Seismological Research Letters* 70: 59-80.
Wells, D. L. & Coppersmith, K. J. 1994. New empirical relationships among magnitude, rupture length, rupture width, rupture area, and surface displacement, *Bulletin of the Seismological Society of America* 84(4): 974-1002.